

Constraints on dark matter-neutrino scattering from the Milky-Way satellites and subhalo modeling for dark acoustic oscillations

Kensuke Akita^{1*} and Shin'ichiro Ando^{2,3†}

¹*Particle Theory and Cosmology Group, Center for Theoretical Physics of the Universe, Institute for Basic Science (IBS), Daejeon, 34126, Korea*

²*GRAPPA Institute, University of Amsterdam, 1098 XH Amsterdam, The Netherlands*

³*Kavli Institute for the Physics and Mathematics of the Universe (Kavli IPMU, WPI), University of Tokyo, Kashiwa, Chiba 277-8583, Japan*

Abstract

The elastic scattering between dark matter (DM) and radiation can potentially explain small-scale observations that the cold dark matter faces as a challenge, as damping density fluctuations via dark acoustic oscillations in the early universe erases small-scale structure. We study a semi-analytical subhalo model for interacting dark matter with radiation, based on the extended Press-Schechter formalism and subhalos' tidal evolution prescription. We also test the elastic scattering between DM and neutrinos using observations of Milky-Way satellites from the Dark Energy Survey and PanSTARRS1. We conservatively impose strong constraints on the DM-neutrino scattering cross section of $\sigma_{\text{DM}-\nu, n} \propto E_\nu^n$ ($n = 0, 2, 4$) at 95% confidence level (CL), $\sigma_{\text{DM}-\nu, 0} < 10^{-32} \text{ cm}^2 (m_{\text{DM}}/\text{GeV})$, $\sigma_{\text{DM}-\nu, 2} < 10^{-43} \text{ cm}^2 (m_{\text{DM}}/\text{GeV})(E_\nu/E_\nu^0)^2$ and $\sigma_{\text{DM}-\nu, 4} < 10^{-54} \text{ cm}^2 (m_{\text{DM}}/\text{GeV})(E_\nu/E_\nu^0)^4$, where E_ν is the neutrino energy and E_ν^0 is the average momentum of relic cosmic neutrinos today, $E_\nu^0 \simeq 6.1 \text{ K}$. By imposing a satellite forming condition, we obtain the strongest upper bounds on the DM-neutrino cross section at 95% CL, $\sigma_{\text{DM}-\nu, 0} < 4 \times 10^{-34} \text{ cm}^2 (m_{\text{DM}}/\text{GeV})$, $\sigma_{\text{DM}-\nu, 2} < 10^{-46} \text{ cm}^2 (m_{\text{DM}}/\text{GeV})(E_\nu/E_\nu^0)^2$ and $\sigma_{\text{DM}-\nu, 4} < 7 \times 10^{-59} \text{ cm}^2 (m_{\text{DM}}/\text{GeV})(E_\nu/E_\nu^0)^4$.

*kensuke8a1@ibs.re.kr

†s.ando@uva.nl

Contents

1	Introduction	1
2	DM-neutrino interactions	3
3	Semi-analytical subhalo model for dark acoustic oscillations	4
3.1	Variance of density fluctuations and window function	5
3.2	Critical overdensity for collapse	5
3.3	Evolution of subhalo structure	6
3.4	Evolution of the number of subhalos	7
4	Comparison with N-body simulations	8
5	Constraints on DM-neutrino scattering	9
5.1	Constraints on DM-neutrino scattering cross sections	9
5.2	Constraints on specific DM-neutrino interactions	11
6	Discussions	13
6.1	Uncertainties of constraints	13
6.2	Comparison with results from astrophysical neutrinos	13
6.3	Comparison with results from the Milky-Way satellites in the literature	15
7	Conclusions	15
A	Fitting formula of critical overdensity	16
B	Comparison with other parametrizations of the smooth-k filter	17
C	Distributions of the number of subhalos	18

1 Introduction

Dark matter (DM) is the most dominant but elusive matter in the universe. The DM mass and interactions beyond gravity still remain a mystery. The standard collisionless cold dark matter (CDM) cosmological model is that DM interacts only gravitationally with other particles. While this model explains the cosmic microwave background (CMB) and large-scale structure (LSS) data [1, 2], it has challenges in explaining observations in the small-scale structure [3] such as the missing satellite [4, 5], core-cusp [6–9] and too-big-to-fail [10, 11] problems. Galaxy formation physics may solve these problems [12–15], but observations on small scales still provide a chance to explore DM scenarios beyond the CDM cosmological model.

Interactions of DM beyond gravity with the Standard Model (SM) (i.e., photons [16–25], neutrinos [23, 26–36] or baryons [19, 37–53]) or dark radiation [54–67] induce damping of the primordial density fluctuations via dark acoustic oscillations (DAO) in the early universe. This collisional damping suppresses structure formation on small scales [68, 69], which can potentially solve the small-scale problems [17, 18, 70]. This leaves characteristic signatures on the cosmic microwave background (CMB) as well as the large-scale structure (LSS). In addition, the resulting suppression reduces the number of DM subhalos in a larger host halo and then observable satellite galaxies, which can be formed within DM subhalos but probably not in all subhalos [12, 71].

In this work, we study the constraints on the elastic scattering cross sections of DM and neutrinos using the latest observational data of Milky-Way satellite galaxies from the Dark Energy Survey (DES) and PanSTARRS1 (PS1) [72, 73].¹ To quickly derive theoretical prediction of the number of Milky-Way satellites, we study and use a modified version of a semi-analytical subhalo model based on the extended Press-Schechter (EPS) formalism [74–77] and subhalos’ tidal evolution prescription, as developed in refs. [78, 79]. The primordial density fluctuations collapse gravitationally, forming DM halos. Halos grow by accreting smaller halos, and the accreted halos are called subhalos. After the accretion of subhalos onto a host halo, they lose mass through gravitational tidal stripping, changing their internal structure [80–82]. The model developed in refs. [78, 79] describes the complementary semi-analytical evolution of a host halo and subhalos, including tidal stripping, with analytical expressions for the hierarchical assembly of DM halos provided by the EPS formalism. In this study, we extend it to interacting dark matter models by modifying the EPS formalism, in particular the window function and the critical overdensity. To obtain the expected number of subhalos, we use a modified version of publicly available SASHIMI codes.^{2 3}

We compare the computed number of Milky-Way satellite galaxies with the observed number of satellite galaxies to constrain the cross section of DM and neutrinos. We use observational data of 270 Milky-Way satellite galaxies from DES and PS1 after completeness correction [72] as well as a subset of 94 satellite galaxies that contain kinematics data. We consider the mass of the Milky-Way halo in the range of $(0.6\text{--}2.0) \times 10^{12} M_{\odot}$, which is determined in refs. [83–86] based on the latest Gaia data. For our conservative constraints, we assume that all the subhalos host satellite galaxies. We also derive stronger limits, imposing a galaxy forming condition in subhalos that reduces the expected number of satellite galaxies.

We find the strongest constraints on the DM-neutrino scattering cross section of $\sigma_{\text{DM}-\nu, n} \propto E_{\nu}^n$ ($n = 0, 2, 4$) at 95% confidence level (CL) in figures 3, 4 and 5, where E_{ν} is the neutrino energy. These results are independent of specific particle physics model. The constraints from CMB [23, 26–28, 32] and Lyman- α forests [27, 34] are also shown in these figures for comparison. To compare with astrophysical constraints from observations of supernova (SN) 1987A neutrinos [26] and high-energy neutrinos [87–94], we need to consider a more specific model rather than the cross sections as discussed in section 6.2.

This paper is organized as follows. In section 2, we review DM-neutrino interactions and their effects on primordial density fluctuations. Section 3 presents our semi-analytical model of subhalo

¹https://github.com/eonadler/subhalo_satellite_connection

²<https://github.com/shinichiroando/sashimi-c>

³<https://github.com/shinichiroando/sashimi-w>

evolution for the DM-radiation interaction scenarios. In section 4, we compare the results of our model with publicly available data of N-body simulations for interacting DM model. In section 5, we show the constraints on the DM-neutrinos cross sections using the presented semi-analytical model and the population data of Milky-Way satellites. In section 6, we discuss uncertainties of our results and compare our constraints with astrophysical ones on the DM-neutrino scattering. Here we also compare our results with the results in the literature. Section 7 concludes the paper. Supplemental materials on our semi-analytical subhalo model are given in appendices A, B and C.

2 DM-neutrino interactions

We consider three types of the scattering cross section of DM and neutrinos, $\sigma_{\text{DM}-\nu}$. One is constant and the others are proportional to neutrino-energy squared and quartered, $\sigma_{\text{DM}-\nu,n} \propto E_\nu^n \propto a^{-n}$ ($n = 0, 2, 4$), where a is the scale factor of the universe normalized to unity today. A constant cross section can be obtained when the DM and mediator masses are strongly degenerate (like Thomson scattering). The cross section would typically depend on neutrino-energy squared or quartered (see appendix C in ref. [87] for the cross sections in specific DM-neutrino interactions).

DM-radiation interactions result in additional collision terms in the perturbation equations for DM and radiation. The modified Euler equations for DM and neutrinos are given by⁴ [26, 27, 95]

$$\dot{\theta}_\nu = k^2\psi + k^2\left(\frac{1}{4}\delta_\nu - \sigma_\nu\right) - \Gamma_{\nu\text{-DM}}(\theta_\nu - \theta_{\text{DM}}), \quad (1)$$

$$\dot{\theta}_{\text{DM}} = k^2\psi - \mathcal{H}\theta_{\text{DM}} - \Gamma_{\text{DM}-\nu}(\theta_{\text{DM}} - \theta_\nu), \quad (2)$$

where θ_ν and θ_{DM} are the velocity divergence for the neutrinos and DM, respectively, k is the comoving wavenumber, ψ is the curvature potential, δ_ν is the neutrino density fluctuation, σ_ν is the neutrino anisotropic stress potential and $\mathcal{H} = (\dot{a}/a)$ is the conformal Hubble parameter. An overdot denotes a derivative with respect to conformal time. The DM-neutrino interactions also modify the Boltzmann hierarchy for neutrinos. For brevity, we do not show the full modified Boltzmann equations for DM and neutrinos [31, 32].

$\Gamma_{\nu\text{-DM}}$ ($\Gamma_{\text{DM}-\nu}$) is the conformal neutrino (DM) collision rate with DM (neutrinos),

$$\Gamma_{\nu\text{-DM}} = a\sigma_{\text{DM}-\nu}n_{\text{DM}}, \quad (3)$$

$$\Gamma_{\text{DM}-\nu} = \frac{4\rho_\nu}{3\rho_{\text{DM}}}\Gamma_{\nu\text{-DM}}, \quad (4)$$

where $n_{\text{DM}} = \rho_{\text{DM}}/m_{\text{DM}}$ is the DM number density and m_{DM} is the DM mass. The unknown parameter of DM in eqs. (3) and (4) is $\sigma_{\text{DM}-\nu}/m_{\text{DM}}$, which can be written as the dimensionless quantity,

$$u_{\text{DM}-\nu,n} \equiv \left[\frac{\sigma_{\text{DM}-\nu,n}}{\sigma_{\text{Th}}}\right] \left[\frac{m_{\text{DM}}}{100 \text{ GeV}}\right]^{-1}, \quad (5)$$

$$u_{\text{DM}-\nu,n} = u_{\text{DM}-\nu,n}^0 a^{-n}, \quad (6)$$

⁴We use the Newtonian gauge and assume massless neutrinos.

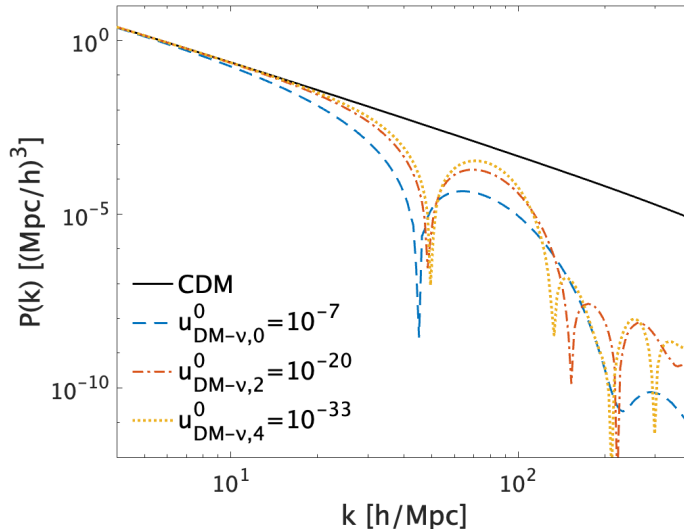


Figure 1: The linear matter power spectra for CDM, the DM-neutrino interaction scenario with $u_{\text{DM}-\nu,0}^0 = 10^{-7}$, $u_{\text{DM}-\nu,2}^0 = 10^{-20}$ and $u_{\text{DM}-\nu,4}^0 = 10^{-33}$, which are defined in eqs. (5) and (6).

where $\sigma_{\text{Th}} = 6.65 \times 10^{-25} \text{ cm}^2$ is the Thomson cross section and $u_{\text{DM}-\nu,n}^0$ is a value of $u_{\text{DM}-\nu,n}$ normalized by relic neutrino momentum today.

In figure 1, we show the effects of DM-neutrino interactions on the linear matter power spectrum. We obtain the matter power spectrum using publicly available modified versions of the Boltzmann code CLASS [96] described in refs. [31,32,97] for DM-neutrino interactions. For higher n , the decoupling time scale is more instantaneous, inducing the higher frequency of oscillations and the flatter spectrum shape.

For the interaction strength of our interest, DM decouples with neutrinos long before recombination [97]. We expect that the DM-neutrino interactions affect only the initial matter power spectrum and have negligible direct effects on the late-time evolution of DM.

Note that we assume the DM energy density behaves as $\rho_{\text{DM}} = \rho_{\text{DM}}^0 a^{-3}$ at the DM-neutrino decoupling epoch, where ρ_{DM}^0 is the DM energy density observed today. As a result, for $m_{\text{DM}} \lesssim 10 \text{ keV}$ with $u_{\text{DM}-\nu}$ of our interest, DM may be enough heated by neutrinos to be relativistic at the DM-neutrino decoupling [97] (see also eq. (44) in appendix A), changing the evolution of ρ_{DM} . We focus on the DM mass of $m_{\text{DM}} \gtrsim 10 \text{ keV}$.

3 Semi-analytical subhalo model for dark acoustic oscillations

To quickly and comprehensively estimate the effects of the suppressed matter power spectrum due to DM-radiation interactions on the number of subhalos via DAO, we consider a modified version of semi-analytical model for subhalo (and host halo) evolution proposed in refs. [78,79]. Our semi-analytical model is similar to the case of WDM particles [79], where the small scale structure is similarly suppressed due to their free streaming, but we modify the EPS formalism, in particular the

window function and the critical overdensity, as described in sections 3.1 and 3.2.

3.1 Variance of density fluctuations and window function

An important ingredient in the semi-analytical model based on the EPS formalism is the linear matter power spectrum characterized by the variance, $S = \sigma^2$ at $z = 0$, where z is the redshift. In the EPS method, the variance has to be spherically smoothed on a mass scale M weighted by a window function $\widetilde{W}(kR)$,

$$S(M) = \sigma^2(M) = \frac{1}{2\pi^2} \int_0^\infty P(k) \widetilde{W}^2(kR) k^2 dk, \quad (7)$$

where $M = M(R)$. $\widetilde{W}(kR)$ needs to be fixed by comparing with N-body simulations. The top-hat filter is a successful choice in the CDM case, while the sharp-k filter successfully reproduces the prediction with N-body simulations for the truncated power spectra such as WDM [98,99]. However, both window functions fail to reproduce the halo abundance in the universe for interacting DM models [65,100] since they cannot properly account for the suppressed power spectrum on small scale. We adopt another window function, called the smooth-k filter proposed in ref. [101],

$$\widetilde{W}^{\text{smooth-k}}(kR) = \frac{1}{1 + (kR)^\beta}, \quad (8)$$

where β is a free parameter that controls the small-scale slope. For $\beta \rightarrow \infty$, the smooth-k filter coincides with the sharp-k filter, $\widetilde{W}^{\text{smooth-k}}(kR) \rightarrow \widetilde{W}^{\text{sharp-k}}(kR) = \Theta(1 - kR)$, where Θ is the Heaviside step function. For large k modes, the smooth-k filter has non-zero values, unlike the sharp-k filter. It successfully reproduces the halo abundance in some models of interacting DM with dark radiation (DR) [65–67], where the matter power spectrum is similar to figure 1.

The mass M associated with the filter scale R is less well defined. We assign the mass M as $M = 4\pi\bar{\rho}(cR)^3/3$, where $\bar{\rho}$ is the average matter density of the universe and c is a free parameter. The parameter set (c, β) must be calibrated using simulations. We adopt $(c, \beta) = (3.7, 3.5)$ [65, 66]. Similar but different choices of (c, β) for interacting DM are also proposed in refs. [67, 101].

3.2 Critical overdensity for collapse

Another important ingredient in the EPS formalism is the critical overdensity δ_c , above which the DM linear density spherically collapses into a halo. In the DM-radiation interaction scenario, radiation may heat DM, producing pressure for DM and delaying the collapse. This may also change the critical overdensity from the CDM case and be similar to the WDM case. However, for $m_{\text{DM}} \gtrsim \text{MeV}$ with the interaction strength of our interest, DM would be heavy enough that we adopt the CDM case to δ_c (see also the detailed discussion in appendix A),

$$\delta_c \simeq \delta_{c,\text{CDM}}(z) \equiv 1.686/D(z), \quad (9)$$

where $D(z)$ is the linear growth factor normalized to unity at $z = 0$. For $m_{\text{DM}} \lesssim \text{MeV}$, using eq. (9) is still a conservative choice.

3.3 Evolution of subhalo structure

After the accretion of subhalos onto the host halo, they lose mass by tidal stripping in the host halo. The average mass-loss rate of subhalos is given by [80]

$$\dot{m}(z) = -A \frac{m(z)}{\tau_{\text{dyn}}(z)} \left[\frac{m(z)}{M(z)} \right]^\zeta, \quad (10)$$

where $m(z)$ and $M(z)$ are the subhalo and host halo masses, respectively, and $\tau_{\text{dyn}}(z)$ is the dynamical timescale [80]. A and ζ are functions of $M(z)$ and z . The mass evolution of the host halo is the same in the CDM and WDM universes [78, 79] because the accretion of larger halos may mainly contribute to the evolution of the host halo. The functions A and ζ are also almost the same in the CDM and WDM universes [78, 79] because the mass evolution of subhalos would mainly depend on the host halo mass. We expect that even for interacting DM models, the subhalo mass evolution is the same with the CDM and WDM cases. We adopt the analytical expression of the host halo evolution $M(z)$ in ref. [102],

$$M(z) = M_0(1+z)^\alpha \exp(\beta z), \quad (11)$$

where

$$\beta = -f(M_0), \quad \alpha = \left[1.686(2/\pi)^{1/2} \frac{dD}{dz} \Big|_{z=0} + 1 \right] f(M_0), \quad (12)$$

with

$$\begin{aligned} f(M_0) &= [S(M_0/q) - S(M_0)]^{-1/2}, \\ q &= 4.137 \tilde{z}_f^{-0.9476}, \\ \tilde{z}_f &= -0.0064(\log_{10} M_0)^2 + 0.0237(\log_{10} M_0) + 1.8827. \end{aligned} \quad (13)$$

$M(z)$ is further generalized to obtain the host halo mass $M(z_i)$ at redshift z_i as [103]

$$M(z) = M(z_i)(1+z-z_i)^\alpha \exp(\beta(z-z_i)). \quad (14)$$

We also adopt the fitting functions of A and ζ proposed in ref. [79],

$$\log A = \left[-0.0019 \log \left(\frac{M(z)}{M_\odot} \right) + 0.045 \right] z + 0.0097 \log \left(\frac{M(z)}{M_\odot} \right) - 0.31, \quad (15)$$

$$\zeta = \left[-0.000056 \log \left(\frac{M(z)}{M_\odot} \right) + 0.0014 \right] z + 0.00033 \log \left(\frac{M(z)}{M_\odot} \right) - 0.0081. \quad (16)$$

We assume the subhalo density profile follows the Navarro-Frenk-White (NFW) profile [104] with a truncation radius r_t due to tidal stripping [105],

$$\rho(r) = \begin{cases} \rho_s r_s^3 / [r(r+r_s)^2], & \text{for } r \leq r_t, \\ 0, & \text{for } r > r_t. \end{cases} \quad (17)$$

We also assume the NFW density profile for (sub)halos before their accretion onto a host halo.

At accretion redshift z_a when the halo becomes a subhalo, we determine the virial radius $r_{\text{vir},a}$ for a subhalo with mass m_a as

$$m_a = \frac{4\pi}{3} \Delta(z_a) \rho_c(z_a) r_{\text{vir},a}^3, \quad (18)$$

where $\Delta = 18\pi^2 + 82d - 39d^2$, $d(z) = \Omega_m(1+z)^3 / [\Omega_m(1+z)^3 + \Omega_\Lambda] - 1$ [106] and $\rho_c(z)$ is the critical density. The scale radius $r_{s,a}$ at z_a is determined as $r_{s,a} = r_{\text{vir},a} / c_{\text{vir},a}$, given a virial concentration parameter $c_{\text{vir},a}$. Then the characteristic density $\rho_{s,a}$ at z_a is obtained by

$$\rho_{s,a} = \frac{m_a}{4\pi r_{s,a}^3 f(c_{\text{vir},a})}, \quad (19)$$

where $f(x) = \ln(1+x) - x/(1+x)$. The suppression of power spectrum on small scales causes DM halos to form later than in the CDM case. The concentration of halos would be lower than the CDM case due to a lower background density owing to cosmic expansion. We adopt the mean values of the concentration parameter obtained in ref. [107]. In ref. [107], the formula for the concentration is applied to CDM and WDM. Recently, ref. [66] confirms that this formula is in a good agreement with simulations in the DM-DR interaction case.

The parameters r_s and ρ_s are related to the maximum circular velocity V_{max} and the corresponding radius r_{max} as

$$r_s = \frac{r_{\text{max}}}{2.163}, \quad \rho_s = \frac{4.625}{4\pi G} \left(\frac{V_{\text{max}}}{r_s} \right)^2. \quad (20)$$

The subhalo structure before and after tidal stripping is related to V_{max} and r_{max} at accretion redshift z_a and any later redshift z_0 [78, 108],

$$\frac{V_{\text{max},0}}{V_{\text{max},a}} = \frac{2^{0.4}(m_0/m_a)^{0.3}}{(1+m_0/m_a)^{0.4}}, \quad \frac{r_{\text{max},0}}{r_{\text{max},a}} = \frac{2^{-0.3}(m_0/m_a)^{0.4}}{(1+m_0/m_a)^{-0.3}}, \quad (21)$$

where m_0 is the subhalo mass at z_0 after tidal stripping. We obtain $r_{s,0}$ and $\rho_{s,0}$ at z_0 through eqs. (20). Then the truncation radius $r_{t,0}$ is obtained by solving

$$m_0 = 4\pi \rho_{s,0} r_{s,0}^3 f\left(\frac{r_{t,0}}{r_{s,0}}\right) \quad (22)$$

and eq. (10). When $r_{t,0}/r_{s,0} < 0.77$, subhalos may be completely disrupted [109], but it has also been pointed out that its complete disruption may not occur [110]. In this work, we take into account its complete tidal disruption.

3.4 Evolution of the number of subhalos

The number of subhalos as a function of mass can be computed as

$$\begin{aligned} \frac{dN_{\text{sh}}}{dm} &= \int dm_a \int dz_a \frac{d^2 N_a}{dm_a dz_a} \int dc_a P(c_a | m_a, z_a) \\ &\quad \times \delta(m - m(m_a, z_a, c_a)) \Theta(r_t(m_a, z_a, c_a) - 0.77 r_s(m_a, z_a, c_a)), \end{aligned} \quad (23)$$

where $\delta(x)$ is the Dirac delta function, c_a are the concentration parameter at accretion redshift z_a and $P(c_a|m_a, z_a)$ is the distribution of c_a . We can calculate the number of subhalos as a function of other quantities such as r_s , ρ_s and V_{\max} by replacing the argument of the delta function in eq. (23) appropriately. For $P(c_a|m_a, z_a)$, we adopt the log-normal function with the mean value $\bar{c}(m_a, z_a)$ [107] and standard deviation of $\sigma_{\log c} = 0.13$ [111].

The number of subhalos accreted onto the main branch of host halo with mass m_a at accretion redshift z_a , $d^2N_a/dm_a dz_a$, can be computed based on the EPS formalism as [112]

$$\frac{d^2N_a}{dm_a dz_a} = \frac{1}{m_a} \mathcal{F}(s_a, \delta_a | S_0, \delta_0; \bar{M}_a) \frac{ds_a}{dm_a} \frac{d\bar{M}_a}{dz_a}, \quad (24)$$

where $\bar{M}_a(z_a)$ is the mean mass of the main branch of host halo at z_a given by eq. (11). $s_a \equiv \sigma^2(m_a)$ and $S_0 \equiv \sigma^2(M_0)$ are the variances of linear matter density on mass scales of m_a and M_0 , respectively. $\delta_a \equiv \delta_c(z_a)$ and $\delta_0 \equiv \delta_c(z_0)$ are the critical overdensities. $\mathcal{F}(s_a, \delta_a | S_0, \delta_0; \bar{M}_a)$ is the fraction of accreted subhalos with mass m_a at z_a in the mass range of the main branch of the host halo $[\bar{M}_a - d\bar{M}_a, \bar{M}_a]$ defined as

$$\mathcal{F}(s_a, \delta_a | S_0, \delta_0; \bar{M}_a) = \int \Phi(s_a, \delta_a | S_0, \delta_0; M_a) P(M_a | S_0, \delta_0) dM_a, \quad (25)$$

with

$$\Phi = \left[\int_{S(m_{\max})}^{\infty} F(s_a, \delta_a | S_0, \delta_0; M_a) ds_a \right]^{-1} \times \begin{cases} F(s_a, \delta_a | S_0, \delta_0; M_a) & \text{if } m_a \geq m_{\max} \\ 0 & \text{if } m_a < m_{\max} \end{cases}, \quad (26)$$

$$F(s_a, \delta_a | S_0, \delta_0; M_a) d \ln \delta_a = \frac{1}{\sqrt{2\pi}} \frac{\delta_a - \delta_M}{(s_a - S_M)^{3/2}} \exp \left[-\frac{(\delta_a - \delta_M)^2}{2(s_a - S_M)} \right], \quad (27)$$

where $P(M_a | S_0, \delta_0)$ is the distribution of the main branch of host halo M_a and $[\dots]^{-1}$ is the normalization factor. $m_{\max} \equiv \min[M_a, M_0/2]$ is the maximum mass of subhalos accreting onto the main branch and $M = M_{\max} \equiv \min[M_a + m_{\max}, M_0]$ is the maximum mass of the main branch of host halo after the mass of the main branch has increased due to the accretion of subhalos with m_a . δ_M are defined at the redshift when the main branch has mass M_{\max} and $S_M = \sigma^2(M_{\max})$.

4 Comparison with N-body simulations

We test our semi-analytical model with numerical simulations. Unfortunately, there is no numerical simulation of subhalo evolution for interacting DM models with neutrinos in the literature. However, there are some results of N-body simulations for subhalo population for interacting DM models with DR [70]. We compare the results from our model with these numerical results. Any radiation would also affect only the initial matter power spectrum directly.

The DM-DR interactions are parametrized by the DM and mediator masses, the abundance of DR and the DM-mediator and DR-mediator couplings. In refs. [59, 70], the effective theory of structure formation (ETHOS) including DM-DR interactions and DM self-interaction is proposed⁵. In the

⁵DM self-interactions would not affect the number of subhalos significantly [70].

following, we focus on ETHOS1-ETHOS3 models, where the above parameters are fixed to concrete values (see ref. [70] for details). In figure 2, we compare the cumulative number of subhalos as a function of maximum circular velocity with the numerical results for the host halo mass of $M_{200} = 1.6 \times 10^{12} M_{\odot}$. We find our model to be in very good agreement with the N-body simulations within a factor of 1.8.

We should note that there are also some results of N-body simulations for the DM-photon interaction scenarios [17, 25]. In ref. [17], the authors compute the number of subhalos as a function of the maximum circular velocity V_{\max} in the mass bin of $(2.3\text{--}2.7) \times 10^{12} M_{\odot}$ but they calculate V_{\max} by the observed stellar line-of-sight velocity dispersions, $V_{\max} = \sqrt{3}\sigma$, which may be underestimated. In ref. [25], the authors compute the number of subhalos as a function of subhalo mass in the large mass bin of $(0.3\text{--}1.4) \times 10^{12} M_{\odot}/h$. Some details of precision of the simulations in refs. [17, 25] are also lower than in the simulations in the case of ETHOS models [70]. Thus, since the simulations in refs. [17, 25] might include relatively large uncertainties, we will not compare our results with them.

Our semi-analytical model is in a very good agreement with the ETHOS models with DM-DR interactions within a factor of 1.8. In addition, our models with the smooth-k filter of different parameter values (c, β) [67, 101] also predict very similar results of figure 2 as discussed in appendix B. These results indicate our model is a valuable tool to explore DM substructure in various interacting DM models quickly. Note that the parameter set of (c, β) in the smooth-k filter is determined to account for the power spectrum on small scale properly. As in figure 1, the small-scale shape of the power spectrum is flatter for higher n of radiation-energy dependence. This indicates that for better predictions of subhalo properties, the parameter set of (c, β) might slightly change, depending on the nature of interactions (interacting species, the radiation-energy dependence of the cross section, the DR abundance, etc).

5 Constraints on DM-neutrino scattering

5.1 Constraints on DM-neutrino scattering cross sections

We compare the expected number of subhalos in the Milky Way obtained by integrating eq. (23) with the observed number of Milky-Way satellite galaxies from DES and PS1 reported in ref. [72]. Ref. [72] corrects the number of detected satellites in DES and PS1 by volumic weights relative to the observable volume. This completeness correction predicts the Milky Way contains 270 satellite galaxies within 300 kpc with absolute V -band magnitude of $M_V < 0$.

We also consider the stellar kinematics data of the Milky-Way satellites. The observed satellite with the smallest line-of-sight velocity dispersion is Leo V with $\sigma = 2.3 \text{ km s}^{-1}$ [113]. Assuming that the velocity dispersion is isotropic, the halo circular velocity of Leo V is $V_{\text{circ}} = \sqrt{3}\sigma = 4 \text{ km s}^{-1}$. We conservatively regard $V_{\text{circ}} = 4 \text{ km s}^{-1}$ as the threshold of maximum circular velocity. In ref. [79], the authors found 94 satellite galaxies with $V_{\max} > 4 \text{ km s}^{-1}$, which contains 82 satellite galaxies after completeness corrections and 12 satellite galaxies without the corrections.

We compute eq. (23) taking 500 logarithmic steps from $m_a = 10M_{\odot}$ to $0.1M_{200}$ in the subhalo mass and steps of $dz = 0.1$ from $z_a = 7$ to 0.1 in redshift, where M_{200} is the Milky-Way halo mass. M_{200} is the mass contained within the radius whose mean density 200 times the critical density. We have confirmed that the results converge enough in these steps. We consider the Milky-Way mass in

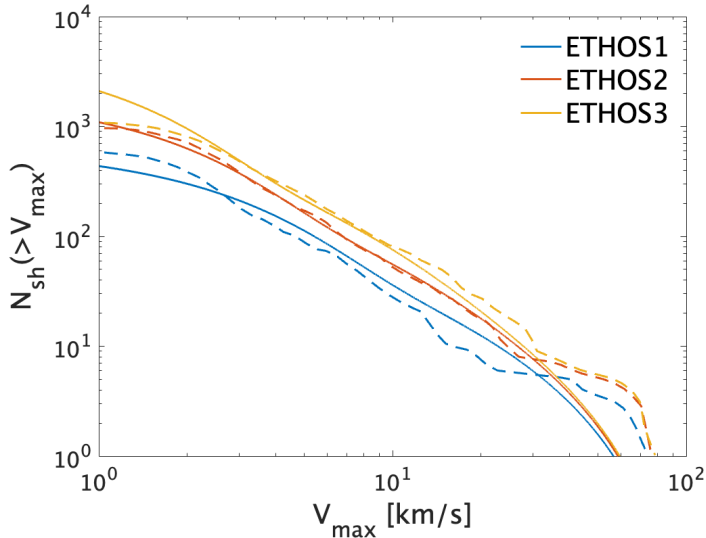


Figure 2: Cumulative number of subhalos as a function of the maximum circular velocity with the host halo mass of $M_{200} = 1.6 \times 10^{12} M_{\odot}$ for DM-DR interaction scenarios (ETHOS1-ETHOS3 models described in ref. [70]). Solid lines denote our results and dashed lines denote the results of N-body simulations from ref. [70].

the range of $M_{200} = (0.6-2.0) \times 10^{12} M_{\odot}$ based on the latest Gaia data [83–86]. To obtain the expected number of subhalos, we modify the publicly available **SASHIMI** code.

To constrain the elastic scattering between DM and neutrinos, we define the Poisson probability of obtaining the observed number of satellites N for the expected number of satellites in our models μ as $P(N|\mu) = \mu^N \exp(-\mu)/N!$. We rule out the elastic scattering of DM and neutrinos at 95% CL when $P(> N_{\text{obs}}|\mu) = \sum_{N=N_{\text{obs}}}^{\infty} P(N|\mu) < 0.05$. For the observational data of satellite galaxies of $N_{\text{obs}} = 270$, $\mu \leq 243$ is ruled out while for the kinematics data of $N_{\text{obs}} = 94$ with $V_{\text{max}} > 4 \text{ km s}^{-1}$, $\mu \leq 78$ is ruled out.

For our conservative constraints, we assume that all subhalos host satellite galaxies and use the kinematics data of 94 Milky-Way satellites with $V_{\text{max}} > 4 \text{ km s}^{-1}$. In figures 3, 4 and 5, we show the upper bounds on the DM-neutrino scattering cross section of $\sigma_{\text{DM}-\nu, n} \propto E_{\nu}^n$ ($n = 0, 2, 4$) at 95% CL as a function of the Milky Way mass, respectively. We constrain the DM-neutrino cross section of $\sigma_{\text{DM}-\nu, 0} < 10^{-32} \text{ cm}^2 (m_{\text{DM}}/\text{GeV})$, $\sigma_{\text{DM}-\nu, 2} < 10^{-43} \text{ cm}^2 (m_{\text{DM}}/\text{GeV})(E_{\nu}/E_{\nu}^0)^2$ and $\sigma_{\text{DM}-\nu, 4} < 10^{-54} \text{ cm}^2 (m_{\text{DM}}/\text{GeV})(E_{\nu}/E_{\nu}^0)^4$, where $E_{\nu}^0 \simeq 3.15T_{\nu}^0 \simeq 6.1 \text{ K}$. E_{ν}^0 and T_{ν}^0 are the average momentum and temperature of relic cosmic neutrinos today, respectively. These constraints are stronger than the constraints from CMB [23, 32] and Lyman- α [34], which are also shown in figures 3 and 4.

More realistically, not all subhalos would host satellite galaxies. An ultraviolet background produced by quasars and stars heats gas in small halos, allowing it to escape from their shallow gravitational potential and suppressing star formation in small halos. Some satellite forming conditions reduce the expected number of satellite galaxies, imposing more stringent upper bounds on the scattering of DM and neutrinos. We adopt a threshold halo mass at accretion of $m_a \simeq 10^8 M_{\odot}$ [12, 71, 114], below

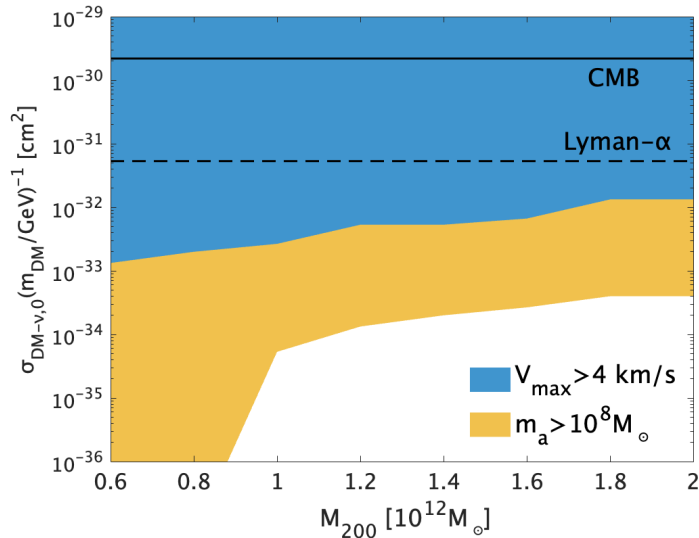


Figure 3: Constraints on the DM-neutrino cross section as $\sigma_{\text{DM}-\nu,0} = \text{const}$ at 95 CL as a function of the Milky-Way mass considering the kinematics data of 94 Milky-Way satellites with $V_{\text{max}} > 4$ km/s (blue) as well as the data of 270 Milky-Way satellites imposing the satellite forming condition of $m_a > 10^8 M_{\odot}$ (yellow). The constraints from CMB (solid line) [23, 32] and Lyman- α (dashed line) [34] are shown for comparison.

which we assume that subhalos do not host satellite galaxies. In this case we can impose the strongest upper bounds of $\sigma_{\text{DM}-\nu,0} < 4 \times 10^{-34} \text{ cm}^2 (m_{\text{DM}}/\text{GeV})$, $\sigma_{\text{DM}-\nu,2} < 10^{-46} \text{ cm}^2 (m_{\text{DM}}/\text{GeV})(E_{\nu}/E_{\nu}^0)^2$ and $\sigma_{\text{DM}-\nu,4} < 7 \times 10^{-59} \text{ cm}^2 (m_{\text{DM}}/\text{GeV})(E_{\nu}/E_{\nu}^0)^4$.

5.2 Constraints on specific DM-neutrino interactions

Following appendix C in ref. [87], we map our strongest constraints to couplings of specific DM-neutrino interactions.⁶ We denote the DM and mediator masses as m_{DM} and m_{ϕ} , respectively. We consider the case of $m_{\phi} \gtrsim m_{\text{DM}} \gg E_{\nu}$.

Scalar DM, scalar mediator:

$$\sigma_{\text{DM}-\nu} \simeq \frac{g^2 g'^2 E_{\nu}^2}{8\pi m_{\text{DM}}^2 m_{\phi}^4}, \quad (28)$$

$$g \lesssim 2 \times 10^{-4} \left(\frac{g'}{\text{MeV}} \right)^{-1} \left(\frac{m_{\text{DM}}}{\text{MeV}} \right)^{3/2} \left(\frac{m_{\phi}}{\text{MeV}} \right)^2 \left(\frac{E_{\nu}}{E_{\nu}^0} \right)^{-1} \left(\frac{\sigma_{\text{DM}-\nu}/m_{\text{DM}}}{10^{-49} \text{ cm}^2/\text{MeV}} \right)^{1/2}. \quad (29)$$

⁶Neutrino telescopes can also constrain couplings of DM-neutrino interactions via DM annihilation to neutrinos [115]. If DM does not annihilate today as in the scenario of asymmetric DM, these constraints are not imposed.

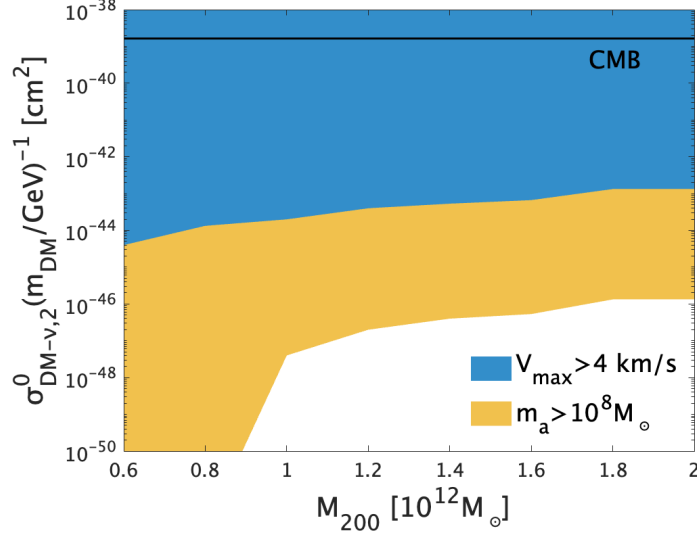


Figure 4: Constraints on the DM-neutrino cross section as $\sigma_{\text{DM}-\nu,2} \propto E_\nu^2$ at 95 CL. $\sigma_{\text{DM}-\nu,2}^0$ is the cross section normalized by relic neutrino momentum today, $\sigma_{\text{DM}-\nu,2} = \sigma_{\text{DM}-\nu,2}^0 (E_\nu/E_\nu^0)^2$. The other details are the same as figure 3.

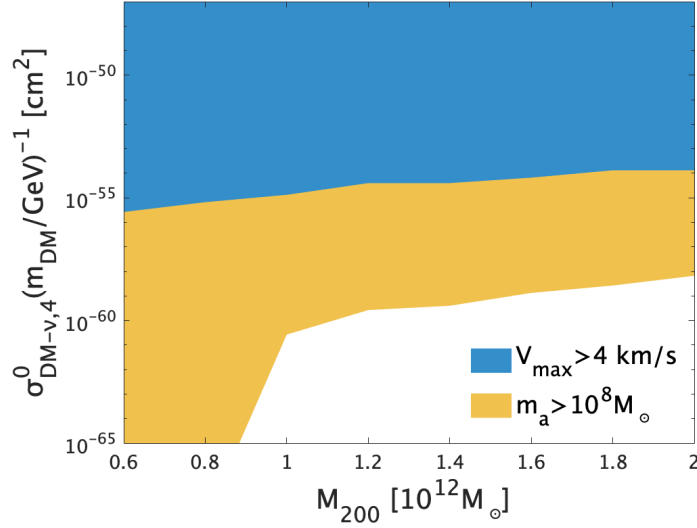


Figure 5: Constraints on the DM-neutrino cross section as $\sigma_{\text{DM}-\nu,4} \propto E_\nu^4$ at 95 CL. $\sigma_{\text{DM}-\nu,4}^0$ is the cross section normalized by relic neutrino momentum today, $\sigma_{\text{DM}-\nu,4} = \sigma_{\text{DM}-\nu,4}^0 (E_\nu/E_\nu^0)^4$. The other details are the same as figure 3.

Dirac fermion DM, scalar/vector mediator:

$$\sigma_{\text{DM}-\nu} \simeq \frac{g^2 g'^2 E_\nu^2}{2\pi m_\phi^4}, \quad (30)$$

$$g \lesssim 8 \times 10^{-5} \left(\frac{g'}{1}\right)^{-1} \left(\frac{m_{\text{DM}}}{\text{MeV}}\right)^{1/2} \left(\frac{m_\phi}{\text{MeV}}\right)^2 \left(\frac{E_\nu}{E_\nu^0}\right)^{-1} \left(\frac{\sigma_{\text{DM}-\nu}/m_{\text{DM}}}{10^{-49} \text{ cm}^2/\text{MeV}}\right)^{1/2}. \quad (31)$$

Scalar DM, fermion mediator:

$$\sigma_{\text{DM}-\nu} \simeq \frac{2g^4 E_\nu^4 m_{\text{DM}}^2}{\pi m_\phi^8}, \quad (32)$$

$$g \lesssim 0.3 \left(\frac{m_{\text{DM}}}{\text{MeV}}\right)^{-1/4} \left(\frac{m_\phi}{\text{MeV}}\right)^2 \left(\frac{E_\nu}{E_\nu^0}\right)^{-1} \left(\frac{\sigma_{\text{DM}-\nu}/m_{\text{DM}}}{7 \times 10^{-62} \text{ cm}^2/\text{MeV}}\right)^{1/4}. \quad (33)$$

Scalar DM, fermion mediator with $m_{\text{DM}} = m_\phi$:

$$\sigma_{\text{DM}-\nu} \simeq \frac{g^4}{8\pi m_{\text{DM}}^2}, \quad (34)$$

$$g \lesssim 4 \times 10^{-4} \left(\frac{m_{\text{DM}}}{\text{MeV}}\right)^{3/4} \left(\frac{\sigma_{\text{DM}-\nu}/m_{\text{DM}}}{4 \times 10^{-37} \text{ cm}^2/\text{MeV}}\right)^{1/4}. \quad (35)$$

6 Discussions

6.1 Uncertainties of constraints

We have used the observational data of 270 Milky-Way satellites after completeness corrections [72]. A companion paper [73] in ref. [72] predicts 220 ± 50 Milky-Way satellites after completeness corrections at 68% confidence level. Adopting 170 Milky-Way satellites, we find that our constraints on the DM-neutrino cross section with a satellite forming condition of $m_a > 10^8 M_\odot$ become weaker by a factor of 3, 40, 6×10^2 for $n = 0, 2, 4$, respectively. Theoretical uncertainties of the completeness corrections are marginalized except for the Milky-Way halo mass. The uncertainty of the Milky-Way halo mass is expected to change the number of the total satellites from 170 to 280 [73], based on the Gaia data of the Milky-Way halo mass.

Our subhalo model coincides with N-body simulations for the ETHOS models with DM-DR interactions within a factor of 1.8 as in figure 2, but the result of cumulative number of satellites on small scales of $V_{\text{max}} \lesssim 10 \text{ km/s}$ by our model is in better agreement with the N-body simulations than a factor of 1.8. This factor might also induce the same order of uncertainties as the above uncertainties.

6.2 Comparison with results from astrophysical neutrinos

Observations of astrophysical neutrinos propagating in DM also constrain the scattering cross sections. Due to the different energy scales of neutrinos, there is no simple mapping to the cross section between cosmological constraints and astrophysical constraints of the DM-neutrino cross sections.

In the following, we consider mainly the DM scattering with high-energy neutrinos [87–94]. We will comment on the constraints from observations of SN 1987A neutrinos in the final paragraph of this section. The most stringent constraints from high energy neutrinos are imposed by neutrino events with $E_\nu \sim 10$ TeV from active galaxy NGC 1068. The upper bounds of the scattering cross section from these events are roughly $\sigma_{\text{DM}-\nu, n} \lesssim 10^{-30} \text{ cm}^2 (m_{\text{DM}}/\text{GeV})(E_\nu/10 \text{ TeV})^n$ [94].⁷

We consider several types of scattering between DM and neutrinos via a mediator particle, following appendix C of ref. [87], and compare with our constraints derived in section 5.2. For scattering of DM with high-energy neutrinos, we consider the parameters of $E_\nu \gg m_\phi \gtrsim m_{\text{DM}}$, where m_ϕ and m_{DM} are the mediator and DM masses, respectively. For $m_\phi \gg E_\nu$ and/or $m_{\text{DM}} \gg E_\nu$, the cross section would be further suppressed by their masses, which is of less interest. We also leave the case of $m_\phi \gg m_{\text{DM}}$ as future work for simplicity. See ref. [87] for a discussion of comparison in the general case. As a result, the constraints on the DM-neutrino scattering cross section from cosmology and high-energy neutrinos are highly complementary.

Scalar DM, scalar mediator:

$$\sigma_{\text{DM}-\nu} \simeq \frac{g^2 g'^2}{64\pi E_\nu^2 m_{\text{DM}}^2} \log \left(\frac{2E_\nu m_{\text{DM}}}{m_\phi^2} \right), \quad (36)$$

$$g \lesssim 5 \times 10^1 \left(\frac{g'}{\text{MeV}} \right)^{-1} \left(\frac{m_{\text{DM}}}{\text{MeV}} \right)^{3/2} \left(\frac{E_\nu}{10 \text{ TeV}} \right) \left(\frac{\sigma_{\text{DM}-\nu}/m_{\text{DM}}}{10^{-33} \text{ cm}^2/\text{MeV}} \right)^{1/2}, \quad (37)$$

where we assume the log term is $\sim \mathcal{O}(10)$. The constraint from high energy neutrinos is weaker than that from the Milky-Way satellite observations, eq. (29).

Dirac fermion DM, scalar mediator:

$$\sigma_{\text{DM}-\nu} \simeq \frac{g^2 g'^2}{32\pi E_\nu m_{\text{DM}}}, \quad (38)$$

$$g \lesssim 5 \times 10^{-2} \left(\frac{g'}{1} \right)^{-1} \left(\frac{m_{\text{DM}}}{\text{MeV}} \right) \left(\frac{E_\nu}{10 \text{ TeV}} \right)^{1/2} \left(\frac{\sigma_{\text{DM}-\nu}/m_{\text{DM}}}{10^{-33} \text{ cm}^2/\text{MeV}} \right)^{1/2}. \quad (39)$$

The above constraint is weaker than that from the Milky-Way satellite observations, eq. (31).

Dirac fermion DM, vector mediator:

$$\sigma_{\text{DM}-\nu} \simeq \frac{g^2 g'^2}{4\pi m_\phi^2}, \quad (40)$$

$$g \lesssim 6 \times 10^{-6} \left(\frac{g'}{1} \right)^{-1} \left(\frac{m_\phi}{\text{MeV}} \right) \left(\frac{m_{\text{DM}}}{\text{MeV}} \right)^{1/2} \left(\frac{\sigma_{\text{DM}-\nu}/m_{\text{DM}}}{10^{-33} \text{ cm}^2/\text{MeV}} \right)^{1/2}. \quad (41)$$

The above constraint is stronger than that from the Milky-Way satellite observations, eq. (31) for $m_\phi \gtrsim m_{\text{DM}} \gtrsim 1 \text{ MeV}$. For $100 \text{ keV} \gtrsim m_\phi \gtrsim m_{\text{DM}}$, eq. (41) is comparable or weaker than eq. (31).

⁷The authors assume DM particles do not annihilate today as in the scenario of asymmetric DM. If DM annihilates, the density of halos through which neutrinos propagate is reduced, weakening this constraint.

Scalar DM, fermion mediator:

$$\sigma_{\text{DM}-\nu} \simeq \frac{g^4}{32\pi E_\nu m_{\text{DM}}} \log\left(\frac{2E_\nu m_{\text{DM}}}{m_\phi^2}\right), \quad (42)$$

$$g \lesssim 0.1 \left(\frac{m_{\text{DM}}}{\text{MeV}}\right)^{1/2} \left(\frac{E_\nu}{10 \text{ TeV}}\right)^{1/4} \left(\frac{\sigma_{\text{DM}-\nu}/m_{\text{DM}}}{10^{-33} \text{ cm}^2/\text{MeV}}\right)^{1/4}, \quad (43)$$

where we assume the log term is $\sim \mathcal{O}(10)$. The above constraint is stronger than that from the Milky-Way satellite observations, eq. (33), for $m_\phi \gtrsim m_{\text{DM}} \gtrsim 1 \text{ MeV}$. For $100 \text{ keV} \gtrsim m_\phi \gtrsim m_{\text{DM}}$, eq. (43) is weaker than eq. (33). In addition, if $m_\phi = m_{\text{DM}}$, eq. (43) is much weaker than that from the Milky-Way satellite observations, eq. (35).

The constraints are also provided by observations of neutrinos from SN 1987A. The thickness of DM through which SN 1987A neutrinos propagate is $\int_8^{50 \text{ kpc}} \rho(r) dr \sim 10^{25} \text{ MeV cm}^{-2}$, where $\rho(r)$ is the DM density in the Milky Way. Then the constraints from SN 1987A observations read $\sigma_{\text{DM}-\nu, n} \lesssim 10^{-25} \text{ cm}^2 (m_{\text{DM}}/\text{MeV})(E_\nu/10 \text{ MeV})^n$ [26], where the average energy of SN 1987A neutrinos is $\sim 10 \text{ MeV}$. In many of the parameter regions of the above examples, the constraints on the couplings from SN 1987A neutrinos are comparable or weaker than those from the Milky-Way satellite or high-energy neutrino observations.

6.3 Comparison with results from the Milky-Way satellites in the literature

Strictly speaking, there is no previous constraint on the DM-neutrino scattering from the Milky-Way satellite observations, but refs. [17, 21] provided the constraints on the DM-photon scattering cross section, which might be similar to the limits on the DM-neutrino cross section. We compare our methods and results with refs. [17, 21].

In ref. [17], using the N-body simulations of subhalos and the kinematics data of 40 Milky-Way satellites with $V_{\text{max}} \geq 8 \text{ km/s}$, the authors constrain the DM-photon constant cross section of $\sigma_{\text{DM}-\gamma} < 2 \times 10^{-33} \text{ cm}^2 (m_{\text{DM}}/\text{GeV})$ for the Milky-Way mass of $2 \times 10^{12} M_\odot$. In the numerical simulations of ref. [17], the maximum circular velocity, V_{max} , is calculated by the stellar line-of-sight velocity dispersion, $V_{\text{max}} = \sqrt{3}\sigma$, which may be underestimated. Then our model predicts a larger number of subhalos than the N-body simulations of ref. [17], weakening the constraints on the DM-radiation scattering cross section.

In ref. [21], using the data of ref. [116] and a semi-analytical model with a satellite galaxy formation condition, the authors constrain the DM-photon constant cross section of $\sigma_{\text{DM}-\gamma} < 3.3 \times 10^{-34} \text{ cm}^2$ for the Milky-Way mass of $2 \times 10^{12} M_\odot$. The constraints from our model are weaker than those of ref. [21], predicting a larger number of subhalos. In addition, our model can calculate the number of subhalos as a function of various quantities while the method of ref. [21] can only calculate that as a function of subhalo mass. Our semi-analytical model is more flexible.

7 Conclusions

In this work, we study a semi-analytical subhalo model for interacting dark matter scenarios, which induce dark acoustic oscillations, based on the EPS formalism including subhalos' tidal evolution.

Using this semi-analytical model, we have provided stringent upper bounds on the elastic scattering of DM and neutrinos from the latest population data of the Milky-Way satellite galaxies by DES and PS1 surveys.

The modifications to our semi-analytical model compared with the model for WDM [79] are only using the smooth-k filter and changing the critical overdensity. Our model is in a reasonable agreement with the publicly available results of N-body simulations for three DM-DR interaction scenarios. This agreement indicates that our model is a simple and powerful tool to study subhalo properties in presence of DAO induced by DM-radiation interactions quickly and comprehensively.

By comparing the data of the Milky-Way satellites from DES and PS1 surveys with the results from our model, we have obtained the constraints on the DM-neutrino scattering cross section of $\sigma_{\text{DM}-\nu, n} \propto E_\nu^n$ ($n = 0, 2, 4$) at 95% CL, $\sigma_{\text{DM}-\nu, 0} < 10^{-32} \text{ cm}^2 (m_{\text{DM}}/\text{GeV})$, $\sigma_{\text{DM}-\nu, 2} < 10^{-43} \text{ cm}^2 (m_{\text{DM}}/\text{GeV})(E_\nu/E_\nu^0)^2$ and $\sigma_{\text{DM}-\nu, 4} < 10^{-54} \text{ cm}^2 (m_{\text{DM}}/\text{GeV})(E_\nu/E_\nu^0)^4$. By imposing a satellite forming condition, we obtain the upper bounds on the DM-neutrino cross section at 95% CL, $\sigma_{\text{DM}-\nu, 0} < 4 \times 10^{-34} \text{ cm}^2 (m_{\text{DM}}/\text{GeV})$, $\sigma_{\text{DM}-\nu, 2} < 10^{-46} \text{ cm}^2 (m_{\text{DM}}/\text{GeV})(E_\nu/E_\nu^0)^2$ and $\sigma_{\text{DM}-\nu, 4} < 7 \times 10^{-59} \text{ cm}^2 (m_{\text{DM}}/\text{GeV})(E_\nu/E_\nu^0)^4$. The results obtained in this analysis are independent of specific particle physics models. In section 5.2, we have mapped their constraints to couplings for specific DM-neutrino interactions.

Acknowledgments

KA is supported by IBS under the project code, IBS-R018-D1. The work of SA was supported by MEXT KAKENHI Grant Numbers, JP20H05850 and JP20H05861.

A Fitting formula of critical overdensity

DM-radiation interactions may affect a critical overdensity for DM collapse, δ_c , due to heating DM and producing pressure for DM particles that prevents their collapse. The collapse of DM with pressure is characterized by the Jeans mass, which is the halo mass for which pressure balances gravity in the linear regime. In the following, we consider DM-neutrino interactions. It is straightforward to apply the following discussions to other DM-radiation interaction scenarios.

DM decouples with neutrinos when $\mathcal{H} \sim \Gamma_{\text{DM}-\nu}$. The decoupling redshift z_{dec} is given by

$$1 + z_{\text{dec}} = \left[4.5 \times 10^{12} \left(\frac{u_{\text{DM}-\nu, n}^0}{10^{-7}} \right)^{-1} \right]^{\frac{1}{2+n}}. \quad (44)$$

The temperature of DM is obtained by, assuming DM is non-relativistic at the decoupling,

$$T_{\text{DM}}(z) = T_\nu^0 \frac{(1+z)^2}{1+z_{\text{dec}}}, \quad (45)$$

where $T_\nu^0 = 1.945 \text{ K}$ is the temperature of relic cosmic neutrinos today. The Jeans mass in the

interacting DM scenario is defined as

$$M_J^{\text{IDM}} \equiv \frac{4\pi}{3} \bar{\rho} \left(\frac{\lambda_J^{\text{IDM}}}{2} \right)^3, \quad (46)$$

$$\lambda_J^{\text{IDM}} = \left(\frac{\pi\gamma T_{\text{DM}}}{G\bar{\rho}m_{\text{DM}}} \right)^{1/2}, \quad (47)$$

where $\gamma = 5/3$ for DM particles and G is the gravitational constant. The Jeans mass can be written,

$$M_J^{\text{IDM}} = 1.3 \times 10^6 M_\odot \left(\frac{1+z}{3000} \right)^{3/2} \left(\frac{T_\nu^0}{2 \text{ K}} \right)^{3/2} \left(\frac{\text{MeV}}{m_{\text{DM}}} \right)^{3/2} \left(\frac{1+z_{\text{dec}}}{10^6} \right)^{-3/2}. \quad (48)$$

After the matter-radiation equality of $z_{\text{eq}} \sim 3000$, the density fluctuations begin to grow as $\propto a$.

In ref. [117], the authors discussed the overcritical density for WDM. Using a model for WDM, where WDM is an adiabatic gas with a gas temperature, $T \propto a^{-2}$, they solved one-dimensional hydrodynamical simulations for spherical collapse with pressure (i.e., with the gas temperature T). The hydrodynamical equations for the WDM model are mathematically identical to those for the DM-radiation interaction scenario. Thus, we can apply the results in ref. [117] to our model. The fitting formula of the critical overdensity for the DM-radiation scenario is, based on refs. [117] and [98],

$$\delta_{c,\text{IDM}}(M, z) = \delta_{c,\text{CDM}}(t) \left\{ h(x) \frac{0.04}{\exp(2.3x)} + [1 - h(x)] \exp \left[\frac{0.31687}{\exp(0.809x)} \right] \right\}, \quad (49)$$

where $x = \log[M/M_J^{\text{IDM}}(z_{\text{eq}})]$ and $h(x) = (1 + \exp[(x + 2.4)/0.1])^{-1}$. For $x \gg 1$, we obtain $\delta_{c,\text{IDM}}(M, z) \simeq \delta_{c,\text{CDM}}(t)$. In section 5, we consider the number of Milky-Way satellites N_{sh} with $V_{\text{max}} \geq 4 \text{ km/s}$ or $m_a \geq 10^8 M_\odot$. The relation between the subhalo mass m and their maximal circular velocity V_{max} in presence of the DM-radiation interactions is still non-trivial, but in the WDM case, which has a truncated power spectrum, $V_{\text{max}} \sim 8 \text{ km/s}$ corresponds to $m \sim 10^8 M_\odot$ [118]. In the interaction strength of our interest with $m_{\text{DM}} \gtrsim \text{MeV}$, we typically obtain $M_J(z_{\text{eq}}) \lesssim 10^6 M_\odot$. To compute N_{sh} with $V_{\text{max}} \geq 4 \text{ km/s}$ or $m_a \geq 10^8 M_\odot$, we expect to be able to approximate

$$\delta_{c,\text{IDM}}(M, z) \simeq \delta_{c,\text{CDM}}(t). \quad (50)$$

We have confirmed this approximation does not affect N_{sh} with $V_{\text{max}} \geq 4 \text{ km/s}$ or $m_a \geq 10^8 M_\odot$ for $m_{\text{DM}} \geq \text{MeV}$ and $u_{\text{DM}-\nu,0}^0 = 10^{-6}$. To compute the properties of smaller subhalos or lighter DM particles, we should use the fitting formula of the critical overdensity given by eq. (49). Eq. (50) is a conservative choice, where the number of subhalos is less suppressed, compared with eq. (49).

B Comparison with other parametrizations of the smooth-k filter

In our fiducial model, we adopt the smooth-k filter with $(c, \beta) = (3.7, 3.5)$ [65,66]. We will compare with other choices of $(c, \beta) = (3.3, 3)$ [67] and $(c, \beta) = (3.3, 4.8)$ [101], which are calibrated by simulations of the halo abundance in the universe for other DAO scenarios.

In figure 6, we show the number of subhalos predicted by our models as a function of the maximum circular velocity V_{max} (left panels) and the virial subhalo mass m_0 (right panels) for ETHOS models.

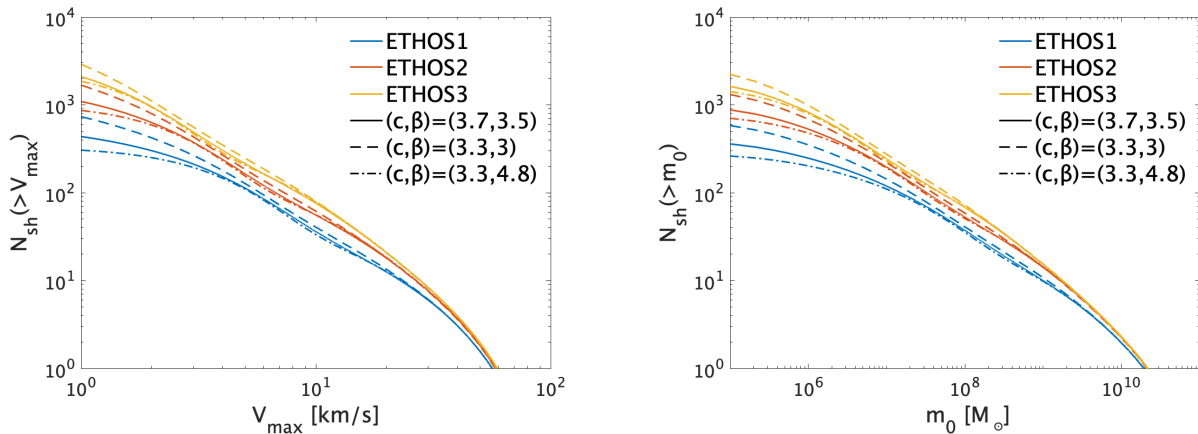


Figure 6: Cumulative number of subhalos as a function of the maximum circular velocity (left) and the virial subhalo mass (right) with the Milky-Way mass of $M_{200} = 1.6 \times 10^{12} M_{\odot}$ for ETHOS models described in ref. [70]. Solid, dashed and dot-dashed lines correspond to our models with the smooth-k filter of parameter values $(c, \beta) = (3.7, 3.5)$ [65, 66], $(3.3, 3)$ [67] and $(3.3, 4.8)$ [101], respectively.

Solid, dashed and dot-dashed lines denote subhalo abundances predicted by the models with $(c, \beta) = (3.7, 3.5)$, $(3.3, 3)$ and $(3.3, 4.8)$, respectively. All models predict almost the same results. Since the different choices of (c, β) are calibrated by simulations of the halo abundance for different DAO scenarios, these results indicate that our fiducial model with $(c, \beta) = (3.7, 3.5)$ can be applied to a broad class of DM-radiation interaction scenarios.

C Distributions of the number of subhalos

In figure 7, we show the number of subhalos predicted by our model as a function of the maximum circular velocity V_{\max} (left panels) and the virial subhalo mass m_0 (right panels) for several examples. In this figure, we consider the constant DM-neutrino cross section for simplicity. We take $u_{\text{DM}-\nu} = 10^{-6}$ (blue lines), $u_{\text{DM}-\nu} = 10^{-7}$ (red lines) and $u_{\text{DM}-\nu} = 10^{-8}$ (yellow lines). In each panel, we assume the Milky-Way mass of $M_{200} = 2.0 \times 10^{12} M_{\odot}$ (top panels), $M_{200} = 1.6 \times 10^{12} M_{\odot}$ (middle panels) and $M_{200} = 0.8 \times 10^{12} M_{\odot}$ (bottom panels).

References

- [1] PLANCK collaboration, *Planck 2018 results. VI. Cosmological parameters*, *Astron. Astrophys.* **641** (2020) A6 [1807.06209].
- [2] eBOSS collaboration, *Completed SDSS-IV extended Baryon Oscillation Spectroscopic Survey: Cosmological implications from two decades of spectroscopic surveys at the Apache Point Observatory*, *Phys. Rev. D* **103** (2021) 083533 [2007.08991].

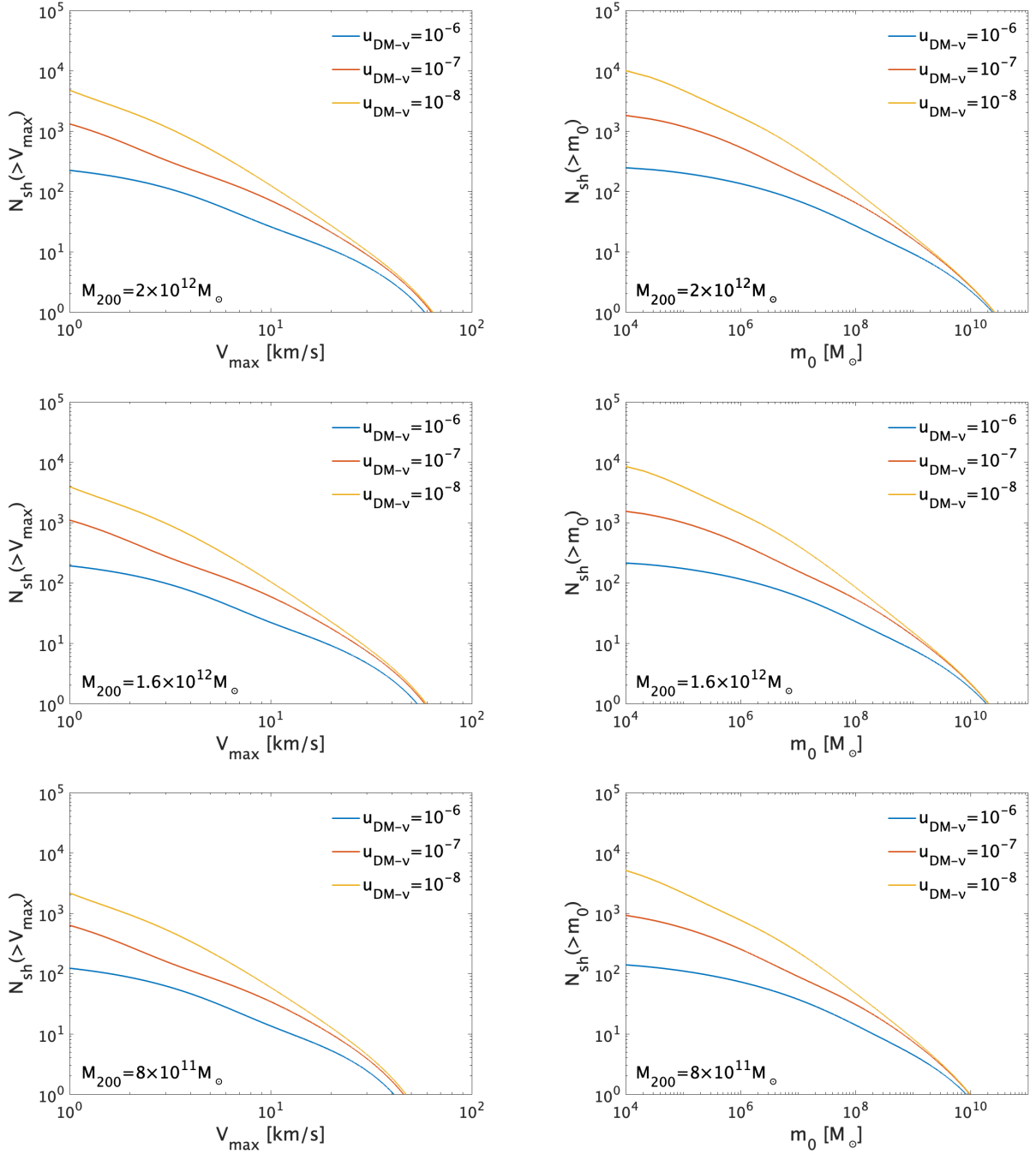


Figure 7: Cumulative number of subhalos as a function of the maximum circular velocity (left) and the virial subhalo mass (right) with the Milky-Way mass of $M_{200} = 2 \times 10^{12} M_{\odot}$ (top), $1.6 \times 10^{12} M_{\odot}$ (middle) and $8 \times 10^{11} M_{\odot}$ (bottom). We consider three DM-neutrino interaction scenarios with the constant DM-neutrino scattering cross section of $u_{\text{DM-}\nu} = 10^{-6}$ (blue lines), $u_{\text{DM-}\nu} = 10^{-7}$ (red lines) and $u_{\text{DM-}\nu} = 10^{-8}$ (yellow lines).

- [3] J.S. Bullock and M. Boylan-Kolchin, *Small-Scale Challenges to the Λ CDM Paradigm*, *Ann. Rev. Astron. Astrophys.* **55** (2017) 343 [[1707.04256](#)].
- [4] A.A. Klypin, A.V. Kravtsov, O. Valenzuela and F. Prada, *Where are the missing Galactic satellites?*, *Astrophys. J.* **522** (1999) 82 [[astro-ph/9901240](#)].
- [5] B. Moore, S. Ghigna, F. Governato, G. Lake, T.R. Quinn, J. Stadel et al., *Dark matter substructure within galactic halos*, *Astrophys. J. Lett.* **524** (1999) L19 [[astro-ph/9907411](#)].
- [6] D.N. Spergel and P.J. Steinhardt, *Observational evidence for selfinteracting cold dark matter*, *Phys. Rev. Lett.* **84** (2000) 3760 [[astro-ph/9909386](#)].
- [7] M.G. Walker and J. Peñarrubia, *A METHOD FOR MEASURING (SLOPES OF) THE MASS PROFILES OF DWARF SPHEROIDAL GALAXIES*, *The Astrophysical Journal* **742** (2011) 20.
- [8] P. Salucci, M.I. Wilkinson, M.G. Walker, G.F. Gilmore, E.K. Grebel, A. Koch et al., *Dwarf spheroidal galaxy kinematics and spiral galaxy scaling laws*, *Mon. Not. Roy. Astron. Soc.* **420** (2012) 2034 [[1111.1165](#)].
- [9] F. Donato, G. Gentile, P. Salucci, C.F. Martins, M.I. Wilkinson, G. Gilmore et al., *A constant dark matter halo surface density in galaxies*, *Monthly Notices of the Royal Astronomical Society* **397** (2009) 1169.
- [10] M. Boylan-Kolchin, J.S. Bullock and M. Kaplinghat, *Too big to fail? the puzzling darkness of massive milky way subhaloes*, *Monthly Notices of the Royal Astronomical Society: Letters* **415** (2011) L40.
- [11] E. Papastergis, R. Giovanelli, M.P. Haynes and F. Shankar, *Is there a “too big to fail” problem in the field?*, *Astron. Astrophys.* **574** (2015) A113 [[1407.4665](#)].
- [12] A.M. Brooks and A. Zolotov, *Why Baryons Matter: The Kinematics of Dwarf Spheroidal Satellites*, *Astrophys. J.* **786** (2014) 87 [[1207.2468](#)].
- [13] J.I. Read, G. Iorio, O. Agertz and F. Fraternali, *The stellar mass-halo mass relation of isolated field dwarfs: a critical test of Λ CDM at the edge of galaxy formation*, *Monthly Notices of the Royal Astronomical Society* (2017) stx147.
- [14] DES collaboration, *Eight Ultra-faint Galaxy Candidates Discovered in Year Two of the Dark Energy Survey*, *Astrophys. J.* **813** (2015) 109 [[1508.03622](#)].
- [15] K.S. Arraki, A. Klypin, S. More and S. Trujillo-Gomez, *Effects of baryon removal on the structure of dwarf spheroidal galaxies*, *Monthly Notices of the Royal Astronomical Society* **438** (2013) 1466.
- [16] R.J. Wilkinson, J. Lesgourgues and C. Boehm, *Using the CMB angular power spectrum to study Dark Matter-photon interactions*, *JCAP* **04** (2014) 026 [[1309.7588](#)].

- [17] C. Boehm, J.A. Schewtschenko, R.J. Wilkinson, C.M. Baugh and S. Pascoli, *Using the Milky Way satellites to study interactions between cold dark matter and radiation*, *Mon. Not. Roy. Astron. Soc.* **445** (2014) L31 [[1404.7012](#)].
- [18] J.A. Schewtschenko, C.M. Baugh, R.J. Wilkinson, C. Boehm, S. Pascoli and T. Sawala, *Dark matter–radiation interactions: the structure of Milky Way satellite galaxies*, *Mon. Not. Roy. Astron. Soc.* **461** (2016) 2282 [[1512.06774](#)].
- [19] Y. Ali-Haïmoud, J. Chluba and M. Kamionkowski, *Constraints on Dark Matter Interactions with Standard Model Particles from Cosmic Microwave Background Spectral Distortions*, *Phys. Rev. Lett.* **115** (2015) 071304 [[1506.04745](#)].
- [20] J. Stadler and C. Boehm, *Constraints on γ -CDM interactions matching the Planck data precision*, *JCAP* **10** (2018) 009 [[1802.06589](#)].
- [21] M. Escudero, L. Lopez-Honorez, O. Mena, S. Palomares-Ruiz and P. Villanueva-Domingo, *A fresh look into the interacting dark matter scenario*, *JCAP* **06** (2018) 007 [[1803.08427](#)].
- [22] S. Kumar, R.C. Nunes and S.K. Yadav, *Cosmological bounds on dark matter-photon coupling*, *Phys. Rev. D* **98** (2018) 043521 [[1803.10229](#)].
- [23] J.A.D. Diacounis and Y.Y.Y. Wong, *On the prior dependence of cosmological constraints on some dark matter interactions*, *JCAP* **05** (2019) 025 [[1811.11408](#)].
- [24] A. Dey, A. Paul and S. Pal, *Constraints on Dark Matter-Neutrino Interaction from 21-cm Cosmology and Forecasts on SKA1-Low*, [2207.02451](#).
- [25] A. Moliné, J.A. Schewtschenko, M.A. Sánchez-Conde, A. Aguirre-Santaella, S.A. Cora and M.G. Abadi, *Properties of subhalos in the interacting dark matter scenario*, *Galaxies* **7** (2019) 80 [[1907.12531](#)].
- [26] G. Mangano, A. Melchiorri, P. Serra, A. Cooray and M. Kamionkowski, *Cosmological bounds on dark matter-neutrino interactions*, *Phys. Rev. D* **74** (2006) 043517 [[astro-ph/0606190](#)].
- [27] R.J. Wilkinson, C. Boehm and J. Lesgourgues, *Constraining Dark Matter-Neutrino Interactions using the CMB and Large-Scale Structure*, *JCAP* **05** (2014) 011 [[1401.7597](#)].
- [28] M. Escudero, O. Mena, A.C. Vincent, R.J. Wilkinson and C. Boehm, *Exploring dark matter microphysics with galaxy surveys*, *JCAP* **09** (2015) 034 [[1505.06735](#)].
- [29] E. Di Valentino, C. Boehm, E. Hivon and F.R. Bouchet, *Reducing the H_0 and σ_8 tensions with Dark Matter-neutrino interactions*, *Phys. Rev. D* **97** (2018) 043513 [[1710.02559](#)].
- [30] A. Olivares-Del Campo, C. Boehm, S. Palomares-Ruiz and S. Pascoli, *Dark matter-neutrino interactions through the lens of their cosmological implications*, *Phys. Rev. D* **97** (2018) 075039 [[1711.05283](#)].

- [31] J. Stadler, C. Boehm and O. Mena, *Comprehensive Study of Neutrino-Dark Matter Mixed Damping*, *JCAP* **08** (2019) 014 [[1903.00540](#)].
- [32] M.R. Mosbech, C. Boehm, S. Hannestad, O. Mena, J. Stadler and Y.Y.Y. Wong, *The full Boltzmann hierarchy for dark matter-massive neutrino interactions*, *JCAP* **03** (2021) 066 [[2011.04206](#)].
- [33] A. Paul, A. Chatterjee, A. Ghoshal and S. Pal, *Shedding light on dark matter and neutrino interactions from cosmology*, *JCAP* **10** (2021) 017 [[2104.04760](#)].
- [34] D.C. Hooper and M. Lucca, *Hints of dark matter-neutrino interactions in Lyman- α data*, *Phys. Rev. D* **105** (2022) 103504 [[2110.04024](#)].
- [35] M.R. Mosbech, C. Boehm and Y.Y.Y. Wong, *Probing dark matter interactions with 21cm observations*, *JCAP* **03** (2023) 047 [[2207.03107](#)].
- [36] P. Brax, C. van de Bruck, E. Di Valentino, W. Giarè and S. Trojanowski, *Extended Analysis of Neutrino-Dark Matter Interactions with Small-Scale CMB Experiments*, [2305.01383](#).
- [37] X.-l. Chen, S. Hannestad and R.J. Scherrer, *Cosmic microwave background and large scale structure limits on the interaction between dark matter and baryons*, *Phys. Rev. D* **65** (2002) 123515 [[astro-ph/0202496](#)].
- [38] A. Melchiorri, A. Polosa and A. Strumia, *New bounds on millicharged particles from cosmology*, *Phys. Lett. B* **650** (2007) 416 [[hep-ph/0703144](#)].
- [39] C. Dvorkin, K. Blum and M. Kamionkowski, *Constraining Dark Matter-Baryon Scattering with Linear Cosmology*, *Phys. Rev. D* **89** (2014) 023519 [[1311.2937](#)].
- [40] J.B. Muñoz, E.D. Kovetz and Y. Ali-Haïmoud, *Heating of Baryons due to Scattering with Dark Matter During the Dark Ages*, *Phys. Rev. D* **92** (2015) 083528 [[1509.00029](#)].
- [41] K. Kadota, T. Sekiguchi and H. Tashiro, *A new constraint on millicharged dark matter from galaxy clusters*, [1602.04009](#).
- [42] J.B. Muñoz and A. Loeb, *Constraints on Dark Matter-Baryon Scattering from the Temperature Evolution of the Intergalactic Medium*, *JCAP* **11** (2017) 043 [[1708.08923](#)].
- [43] V. Gluscevic and K.K. Boddy, *Constraints on Scattering of keV–TeV Dark Matter with Protons in the Early Universe*, *Phys. Rev. Lett.* **121** (2018) 081301 [[1712.07133](#)].
- [44] K.K. Boddy and V. Gluscevic, *First Cosmological Constraint on the Effective Theory of Dark Matter-Proton Interactions*, *Phys. Rev. D* **98** (2018) 083510 [[1801.08609](#)].
- [45] W.L. Xu, C. Dvorkin and A. Chael, *Probing sub-GeV Dark Matter-Baryon Scattering with Cosmological Observables*, *Phys. Rev. D* **97** (2018) 103530 [[1802.06788](#)].
- [46] R. Barkana, *Possible interaction between baryons and dark-matter particles revealed by the first stars*, *Nature* **555** (2018) 71 [[1803.06698](#)].

- [47] T.R. Slatyer and C.-L. Wu, *Early-Universe constraints on dark matter-baryon scattering and their implications for a global 21 cm signal*, *Phys. Rev. D* **98** (2018) 023013 [[1803.09734](#)].
- [48] J.B. Muñoz, C. Dvorkin and A. Loeb, *21-cm Fluctuations from Charged Dark Matter*, *Phys. Rev. Lett.* **121** (2018) 121301 [[1804.01092](#)].
- [49] K.K. Boddy, V. Gluscevic, V. Poulin, E.D. Kovetz, M. Kamionkowski and R. Barkana, *Critical assessment of CMB limits on dark matter-baryon scattering: New treatment of the relative bulk velocity*, *Phys. Rev. D* **98** (2018) 123506 [[1808.00001](#)].
- [50] E.O. Nadler, V. Gluscevic, K.K. Boddy and R.H. Wechsler, *Constraints on Dark Matter Microphysics from the Milky Way Satellite Population*, *Astrophys. J. Lett.* **878** (2019) 32 [[1904.10000](#)].
- [51] DES collaboration, *Milky Way Satellite Census. III. Constraints on Dark Matter Properties from Observations of Milky Way Satellite Galaxies*, *Phys. Rev. Lett.* **126** (2021) 091101 [[2008.00022](#)].
- [52] K. Maamari, V. Gluscevic, K.K. Boddy, E.O. Nadler and R.H. Wechsler, *Bounds on velocity-dependent dark matter-proton scattering from Milky Way satellite abundance*, *Astrophys. J. Lett.* **907** (2021) L46 [[2010.02936](#)].
- [53] K.K. Rogers, C. Dvorkin and H.V. Peiris, *Limits on the Light Dark Matter–Proton Cross Section from Cosmic Large-Scale Structure*, *Phys. Rev. Lett.* **128** (2022) 171301 [[2111.10386](#)].
- [54] R. Diamanti, E. Giusarma, O. Mena, M. Archidiacono and A. Melchiorri, *Dark Radiation and interacting scenarios*, *Phys. Rev. D* **87** (2013) 063509 [[1212.6007](#)].
- [55] F.-Y. Cyr-Racine, R. de Putter, A. Raccanelli and K. Sigurdson, *Constraints on Large-Scale Dark Acoustic Oscillations from Cosmology*, *Phys. Rev. D* **89** (2014) 063517 [[1310.3278](#)].
- [56] X. Chu and B. Dasgupta, *Dark Radiation Alleviates Problems with Dark Matter Halos*, *Phys. Rev. Lett.* **113** (2014) 161301 [[1404.6127](#)].
- [57] M.A. Buen-Abad, G. Marques-Tavares and M. Schmaltz, *Non-Abelian dark matter and dark radiation*, *Phys. Rev. D* **92** (2015) 023531 [[1505.03542](#)].
- [58] J. Lesgourgues, G. Marques-Tavares and M. Schmaltz, *Evidence for dark matter interactions in cosmological precision data?*, *JCAP* **02** (2016) 037 [[1507.04351](#)].
- [59] F.-Y. Cyr-Racine, K. Sigurdson, J. Zavala, T. Bringmann, M. Vogelsberger and C. Pfrommer, *ETHOS—an effective theory of structure formation: From dark particle physics to the matter distribution of the Universe*, *Phys. Rev. D* **93** (2016) 123527 [[1512.05344](#)].
- [60] R. Foot and S. Vagnozzi, *Solving the small-scale structure puzzles with dissipative dark matter*, *JCAP* **07** (2016) 013 [[1602.02467](#)].

- [61] R. Krall, F.-Y. Cyr-Racine and C. Dvorkin, *Wandering in the Lyman-alpha Forest: A Study of Dark Matter-Dark Radiation Interactions*, *JCAP* **09** (2017) 003 [[1705.08894](#)].
- [62] M. Archidiacono, S. Bohr, S. Hannestad, J.H. Jørgensen and J. Lesgourgues, *Linear scale bounds on dark matter–dark radiation interactions and connection with the small scale crisis of cold dark matter*, *JCAP* **11** (2017) 010 [[1706.06870](#)].
- [63] M.A. Buen-Abad, M. Schmaltz, J. Lesgourgues and T. Brinckmann, *Interacting Dark Sector and Precision Cosmology*, *JCAP* **01** (2018) 008 [[1708.09406](#)].
- [64] M. Archidiacono, D.C. Hooper, R. Murgia, S. Bohr, J. Lesgourgues and M. Viel, *Constraining Dark Matter-Dark Radiation interactions with CMB, BAO, and Lyman- α* , *JCAP* **10** (2019) 055 [[1907.01496](#)].
- [65] O. Sameie, A.J. Benson, L.V. Sales, H.-B. Yu, L.A. Moustakas and P. Creasey, *The Effect of Dark Matter–Dark Radiation Interactions on Halo Abundance: A Press–Schechter Approach*, *Astrophys. J.* **874** (2019) 101 [[1810.11040](#)].
- [66] S. Bohr, J. Zavala, F.-Y. Cyr-Racine and M. Vogelsberger, *The halo mass function and inner structure of ETHOS haloes at high redshift*, *Mon. Not. Roy. Astron. Soc.* **506** (2021) 128 [[2101.08790](#)].
- [67] T. Schaeffer and A. Schneider, *Dark acoustic oscillations: imprints on the matter power spectrum and the halo mass function*, *Mon. Not. Roy. Astron. Soc.* **504** (2021) 3773 [[2101.12229](#)].
- [68] C. Boehm, P. Fayet and R. Schaeffer, *Constraining dark matter candidates from structure formation*, *Phys. Lett. B* **518** (2001) 8 [[astro-ph/0012504](#)].
- [69] C. Boehm and R. Schaeffer, *Constraints on dark matter interactions from structure formation: Damping lengths*, *Astron. Astrophys.* **438** (2005) 419 [[astro-ph/0410591](#)].
- [70] M. Vogelsberger, J. Zavala, F.-Y. Cyr-Racine, C. Pfrommer, T. Bringmann and K. Sigurdson, *ETHOS – an effective theory of structure formation: dark matter physics as a possible explanation of the small-scale CDM problems*, *Mon. Not. Roy. Astron. Soc.* **460** (2016) 1399 [[1512.05349](#)].
- [71] T. Sawala et al., *The chosen few: the low-mass haloes that host faint galaxies*, *Mon. Not. Roy. Astron. Soc.* **456** (2016) 85 [[1406.6362](#)].
- [72] DES collaboration, *Milky Way Satellite Census. I. The Observational Selection Function for Milky Way Satellites in DES Y3 and Pan-STARRS DR1*, *Astrophys. J.* **893** (2020) 1 [[1912.03302](#)].
- [73] DES collaboration, *Milky Way Satellite Census – II. Galaxy-Halo Connection Constraints Including the Impact of the Large Magellanic Cloud*, *Astrophys. J.* **893** (2020) 48 [[1912.03303](#)].

- [74] W.H. Press and P. Schechter, *Formation of galaxies and clusters of galaxies by selfsimilar gravitational condensation*, *Astrophys. J.* **187** (1974) 425.
- [75] J.R. Bond, S. Cole, G. Efstathiou and N. Kaiser, *Excursion set mass functions for hierarchical Gaussian fluctuations*, *Astrophys. J.* **379** (1991) 440.
- [76] R.G. Bower, *The Evolution of groups of galaxies in the Press-Schechter formalism*, *Mon. Not. Roy. Astron. Soc.* **248** (1991) 332.
- [77] C.G. Lacey and S. Cole, *Merger rates in hierarchical models of galaxy formation*, *Mon. Not. Roy. Astron. Soc.* **262** (1993) 627.
- [78] N. Hiroshima, S. Ando and T. Ishiyama, *Modeling evolution of dark matter substructure and annihilation boost*, *Phys. Rev. D* **97** (2018) 123002 [[1803.07691](#)].
- [79] A. Dekker, S. Ando, C.A. Correa and K.C.Y. Ng, *Warm dark matter constraints using Milky Way satellite observations and subhalo evolution modeling*, *Phys. Rev. D* **106** (2022) 123026 [[2111.13137](#)].
- [80] F. Jiang and F.C. van den Bosch, *Statistics of dark matter substructure – I. Model and universal fitting functions*, *Mon. Not. Roy. Astron. Soc.* **458** (2016) 2848 [[1403.6827](#)].
- [81] F.C. van den Bosch, G. Tormen and C. Giocoli, *The Mass function and average mass loss rate of dark matter subhaloes*, *Mon. Not. Roy. Astron. Soc.* **359** (2005) 1029 [[astro-ph/0409201](#)].
- [82] C. Giocoli, G. Tormen and F.C.v.d. Bosch, *The Population of Dark Matter Subhaloes: Mass Functions and Average Mass Loss Rates*, *Mon. Not. Roy. Astron. Soc.* **386** (2008) 2135 [[0712.1563](#)].
- [83] E.V. Karukes, M. Benito, F. Iocco, R. Trotta and A. Geringer-Sameth, *A robust estimate of the Milky Way mass from rotation curve data*, *JCAP* **05** (2020) 033 [[1912.04296](#)].
- [84] L. Posti and A. Helmi, *Mass and shape of the milky way’s dark matter halo with globular clusters from gaia and hubble*, *Astronomy & Astrophysics* **621** (2019) A56.
- [85] G. Eadie and M. Jurić, *The cumulative mass profile of the milky way as determined by globular cluster kinematics from gaia DR2*, *The Astrophysical Journal* **875** (2019) 159.
- [86] T.K. Fritz, G. Battaglia, M.S. Pawlowski, N. Kallivayalil, R. van der Marel, S.T. Sohn et al., *Gaia DR2 proper motions of dwarf galaxies within 420 kpc*, *Astronomy & Astrophysics* **619** (2018) A103.
- [87] C.A. Argüelles, A. Kheirandish and A.C. Vincent, *Imaging Galactic Dark Matter with High-Energy Cosmic Neutrinos*, *Phys. Rev. Lett.* **119** (2017) 201801 [[1703.00451](#)].
- [88] S. Pandey, S. Karmakar and S. Rakshit, *Interactions of astrophysical neutrinos with dark matter: a model building perspective*, *JHEP* **01** (2019) 095 [[1810.04203](#)].

- [89] J.B.G. Alvey and M. Fairbairn, *Linking Scalar Dark Matter and Neutrino Masses with IceCube 170922A*, *JCAP* **07** (2019) 041 [[1902.01450](#)].
- [90] K.-Y. Choi, J. Kim and C. Rott, *Constraining dark matter-neutrino interactions with IceCube-170922A*, *Phys. Rev. D* **99** (2019) 083018 [[1903.03302](#)].
- [91] K. Murase and I.M. Shoemaker, *Neutrino Echoes from Multimessenger Transient Sources*, *Phys. Rev. Lett.* **123** (2019) 241102 [[1903.08607](#)].
- [92] J.M. Cline, S. Gao, F. Guo, Z. Lin, S. Liu, M. Puel et al., *Blazar Constraints on Neutrino-Dark Matter Scattering*, *Phys. Rev. Lett.* **130** (2023) 091402 [[2209.02713](#)].
- [93] F. Ferrer, G. Herrera and A. Ibarra, *New constraints on the dark matter-neutrino and dark matter-photon scattering cross sections from TXS 0506+056*, [2209.06339](#).
- [94] J.M. Cline and M. Puel, *NGC 1068 constraints on neutrino-dark matter scattering*, [2301.08756](#).
- [95] C. Boehm, A. Riazuelo, S.H. Hansen and R. Schaeffer, *Interacting dark matter disguised as warm dark matter*, *Phys. Rev. D* **66** (2002) 083505 [[astro-ph/0112522](#)].
- [96] D. Blas, J. Lesgourgues and T. Tram, *The Cosmic Linear Anisotropy Solving System (CLASS) II: Approximation schemes*, *JCAP* **07** (2011) 034 [[1104.2933](#)].
- [97] N. Becker, D.C. Hooper, F. Kahlhoefer, J. Lesgourgues and N. Schöneberg, *Cosmological constraints on multi-interacting dark matter*, *JCAP* **02** (2021) 019 [[2010.04074](#)].
- [98] A.J. Benson, A. Farahi, S. Cole, L.A. Moustakas, A. Jenkins, M. Lovell et al., *Dark Matter Halo Merger Histories Beyond Cold Dark Matter: I - Methods and Application to Warm Dark Matter*, *Mon. Not. Roy. Astron. Soc.* **428** (2013) 1774 [[1209.3018](#)].
- [99] M.R. Lovell, S. Bose, A. Boyarsky, S. Cole, C.S. Frenk, V. Gonzalez-Perez et al., *Satellite galaxies in semi-analytic models of galaxy formation with sterile neutrino dark matter*, *Mon. Not. Roy. Astron. Soc.* **461** (2016) 60 [[1511.04078](#)].
- [100] J.A. Schewtschenko, R.J. Wilkinson, C.M. Baugh, C. Boehm and S. Pascoli, *Dark matter–radiation interactions: the impact on dark matter haloes*, *Mon. Not. Roy. Astron. Soc.* **449** (2015) 3587 [[1412.4905](#)].
- [101] M. Leo, C.M. Baugh, B. Li and S. Pascoli, *A new smooth- k space filter approach to calculate halo abundances*, *JCAP* **04** (2018) 010 [[1801.02547](#)].
- [102] C.A. Correa, J.S.B. Wyithe, J. Schaye and A.R. Duffy, *The accretion history of dark matter haloes – I. The physical origin of the universal function*, *Mon. Not. Roy. Astron. Soc.* **450** (2015) 1514 [[1409.5228](#)].

- [103] C.A. Correa, J.S.B. Wyithe, J. Schaye and A.R. Duffy, *The accretion history of dark matter haloes – III. A physical model for the concentration–mass relation*, *Mon. Not. Roy. Astron. Soc.* **452** (2015) 1217 [[1502.00391](#)].
- [104] J.F. Navarro, C.S. Frenk and S.D.M. White, *A Universal density profile from hierarchical clustering*, *Astrophys. J.* **490** (1997) 493 [[astro-ph/9611107](#)].
- [105] V. Springel, J. Wang, M. Vogelsberger, A. Ludlow, A. Jenkins, A. Helmi et al., *The Aquarius Project: the subhalos of galactic halos*, *Mon. Not. Roy. Astron. Soc.* **391** (2008) 1685 [[0809.0898](#)].
- [106] G.L. Bryan and M.L. Norman, *Statistical properties of x-ray clusters: Analytic and numerical comparisons*, *Astrophys. J.* **495** (1998) 80 [[astro-ph/9710107](#)].
- [107] A.D. Ludlow, S. Bose, R.E. Angulo, L. Wang, W.A. Hellwing, J.F. Navarro et al., *The mass–concentration–redshift relation of cold and warm dark matter haloes*, *Mon. Not. Roy. Astron. Soc.* **460** (2016) 1214 [[1601.02624](#)].
- [108] J. Peñarrubia, A.J. Benson, M.G. Walker, G. Gilmore, A.W. McConnachie and L. Mayer, *The impact of dark matter cusps and cores on the satellite galaxy population around spiral galaxies*, *Monthly Notices of the Royal Astronomical Society* (2010) no.
- [109] E. Hayashi, J.F. Navarro, J.E. Taylor, J. Stadel and T.R. Quinn, *The Structural evolution of substructure*, *Astrophys. J.* **584** (2003) 541 [[astro-ph/0203004](#)].
- [110] F.C. van den Bosch, G. Ogiya, O. Hahn and A. Burkert, *Disruption of Dark Matter Substructure: Fact or Fiction?*, *Mon. Not. Roy. Astron. Soc.* **474** (2018) 3043 [[1711.05276](#)].
- [111] T. Ishiyama, J. Makino, S. Portegies Zwart, D. Groen, K. Nitadori, S. Rieder et al., *The Cosmogrid Simulation: Statistical Properties of Small Dark Matter Halos*, *Astrophys. J.* **767** (2013) 146 [[1101.2020](#)].
- [112] X. Yang, H.J. Mo, Y. Zhang and F.C.v.d. Bosch, *An analytical model for the accretion of dark matter subhalos*, *Astrophys. J.* **741** (2011) 13 [[1104.1757](#)].
- [113] J.D. Simon, *The Faintest Dwarf Galaxies*, *Ann. Rev. Astron. Astrophys.* **57** (2019) 375 [[1901.05465](#)].
- [114] A. Schneider, *Structure formation with suppressed small-scale perturbations*, *Mon. Not. Roy. Astron. Soc.* **451** (2015) 3117 [[1412.2133](#)].
- [115] C.A. Argüelles, A. Diaz, A. Kheirandish, A. Olivares-Del-Campo, I. Safa and A.C. Vincent, *Dark matter annihilation to neutrinos*, *Rev. Mod. Phys.* **93** (2021) 035007 [[1912.09486](#)].
- [116] O. Newton, M. Cautun, A. Jenkins, C.S. Frenk and J. Helly, *The total satellite population of the Milky Way*, *Mon. Not. Roy. Astron. Soc.* **479** (2018) 2853 [[1708.04247](#)].

- [117] R. Barkana, Z. Haiman and J.P. Ostriker, *Constraints on warm dark matter from cosmological reionization*, *Astrophys. J.* **558** (2001) 482 [[astro-ph/0102304](#)].
- [118] M.R. Lovell, C.S. Frenk, V.R. Eke, A. Jenkins, L. Gao and T. Theuns, *The properties of warm dark matter haloes*, *Mon. Not. Roy. Astron. Soc.* **439** (2014) 300 [[1308.1399](#)].